ELEKTRİK, VOL.6, NO.3, 1998, ©TÜBİTAK

# Use of the magnetic field generated by the internal distribution of injected currents for Electrical Impedance Tomography (MR-EIT)

**Y. Ziya İder & Özlem Birgül**
*Middle East Technical University,*
*Department of Electrical and Electronics Engineering,*
*06531, Ankara-TURKEY*
*email: ideryz@ed.eee.metu.edu.tr*

**Abstract**

*In two dimensional conventional Electrical Impedance Tomography (EIT), volume conductor is probed by means of injected currents, and peripheral voltage measurements are used as input to the reconstruction algorithm. The current that flows in the 2D object creates magnetic fields that are perpendicular to the plane of imaging. Such magnetic fields can be measured using magnetic resonance tomography. In this study, use of this magnetic field generated by the injected currents, for the purpose of reconstructing the conductivity distribution, is studied. Sensitivity matrix relating the magnetic field to the element conductivities is calculated using the Finite Element Method and Biot-Savart law. Linearization is made during sensitivity matrix formation. This matrix is inverted using singular value decompostion. Simulations for objects placed in different parts of the imaging region are made to understand the spatial dependency of the proposed method and it is seen that the method has uniform sensitivity throughout the imaging region. Finally, images reconstructed using data taken from an experimental phantom are presented.*

## 1. Introduction

The purpose of medical imaging, or medical tomography, is to display the distribution of a certain property of the tissues of the body. In electrical impedance tomography (EIT) inner distribution of conductivity of an object is obtained by measuring and processing boundary voltage values which result from currents injected into or induced in the object [1]-[5]. However, boundary voltage measurements are not as sensitive to the perturbation of conductivity values of regions distant from the boundary as they are to the perturbations near the boundary. Consequently, spatial resolution of EIT images is less for inner regions than for peripheral regions. The method proposed in this study (MR-EIT) aims at obtaining high spatial resolution uniformly throughout the imaging region.

It has been shown that magnetic fields generated by currents flowing in the body at frequencies used in EIT systems can be measured throughout the whole imaging region using magnetic resonance imaging techniques [8, 10, 16].

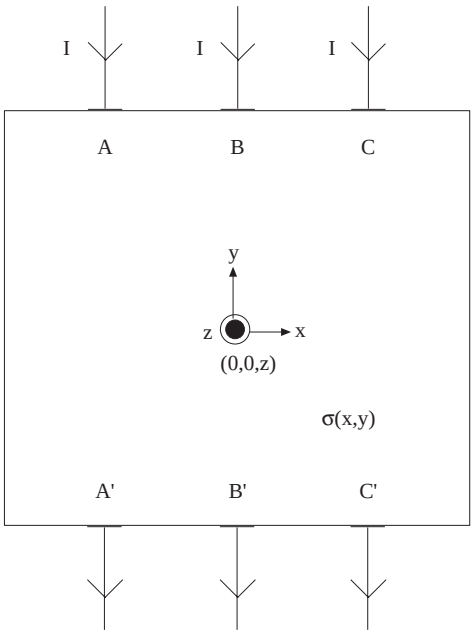


**Figure 1.** Definition of the object used in simulation and experimental studies. The length and width of the object is 9cm and 8.5cm respectively. The depth of the experimental phantom is 1.3cm.

When the inner conductivity is perturbed, the current distribution is altered and a perturbation in the generated magnetic field is observed. Therefore, if this perturbation in the magnetic field can be measured, then an inverse problem may be solved to find the conductivity perturbation [12, 13]. In addition, since the magnetic field perturbation can be measured with equal sensitivity throughout the whole imaging region, then possibly, a conductivity image with uniform spatial resolution may be obtained. In this way, the main disadvantage of injected and induced current EIT systems which stems from the problem of lower sensitivity of peripheral measurements to inner conductivity measurements will be eliminated [14, 15].

This study covers a 2-dimensional (2D) version of the proposed method. The currents that flow in a 2D object, generate a 3D magnetic field. However, on the surface of the object this magnetic field has only a normal component (taken as z-direction in this study). In this study, the relation of the z-component of the magnetic field to inner conductivity perturbations is analysed; sensitivity patterns and matrix are calculated; the behaviour of this matrix is investigated and representative images using simulated data are obtained. Finally, the method is applied to magnetic field measurements obtained using the phantom explained in Figure 1. The current is injected using three pairs of electrodes. Using this configuration a current density which is almost uniform in the imaging region is obtained. The reason for using a uniform current distribution is to obtain similar magnetic field perturbations for conductivity perturbation at any location of the phantom. Simulation studies are also based on the properties and dimensions of this phantom.

# 2. Forward and Inverse Problems

## 2.1. Definitions of Forward and Inverse Problems

Forward problem is defined as calculation of magnetic field generated by the internal current pattern for a given boundary injected current profile and known conductivity distribution. Forward problem formulation is used to supply simulation data to test the proposed reconstruction algorithm and it is also used in

formulating the inverse problem. Inverse problem is to obtain the conductivity distribution in the imaging region using the measured magnetic field distribution.

In the next two sub-sections, formulations and solutions of forward and inverse problems will be given.

## 2.2. Formulation and Solution of the Forward Problem

The first step of the forward problem is the solution of potential field inside the object for a given conductivity distribution and current injection profile. The relation between conductivity and potential field is given by the following equation and the related boundary conditions:

$$\bigtriangledown\cdot(\sigma\,(x,y)\bigtriangledown\phi\,(x,y)\,)=0 \qquad\qquad (x,y)\in S \tag{1}$$

$$\sigma\,(x,y)\,\frac{\partial\phi}{\partial n}=\begin{cases} J & \text{on positive current electrode} \\ -J & \text{on negative current electrode} \\ 0 & \text{elsewhere} \end{cases} \tag{2}$$

where $\sigma$ is the electrical conductivity distribution on $S$, $\phi$ is the electrical potential distribution on $S$ and $S$ is the slice of object to be imaged. After finding the potential distribution by solving the above equation with a suitable technique, electric field and current density distributions are calculated using

$$\vec{E}=-\bigtriangledown\phi \tag{3}$$

and

$$\vec{J}=\sigma\vec{E} \tag{4}$$

respectively.

Equation (1) is non-linear in conductivity and analytical expression for the solution of potential does not exist in general. For this reason, some numerical techniques are to be used. In this study Finite Element Method (FEM) is used to solve the potential distribution for a 2-dimensional case. The FEM mesh (Figure 2) used is composed of 256 nodes and 450 first order triangular elements. The potential field inside an element is assumed to change linearly and is expressed in terms of node potentials and shape functions [9]. For each element conductivity is assumed to be constant.

Using FEM a matrix equation of the form

$$\mathbf{A}\phi=\mathbf{c} \tag{5}$$

is obtained where $\phi$ $(256\times 1)$ is the vector containing unknown node potential values, $\mathbf{A}$ $(256\times 256)$ is the coefficient matrix which depends on mesh properties and also on $\sigma$ $(450\times 1)$, and $\mathbf{c}$ $(256\times 1)$ is the boundary condition vector. $\sigma$ is the vector of conductivity values assigned to the FEM elements. Since potential field is assumed to change linearly within an element, the electric field is found to be constant in an element when gradient operator is applied. Current density values for each element are simply calculated by multiplying the electric field in each element with the corresponding conductivity value.

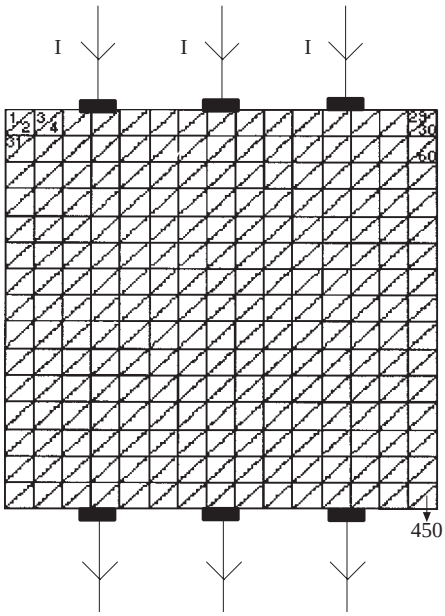


**Figure 2.** The finite element mesh used in potential field calculations. The mesh is composed of 256 nodes and 450 first order triangular elements.

Finally, Biot-Savart law is used to find the magnetic field, $\vec{B}$, generated by the current density calculated above. For the $i^{th}$ element, current density is multiplied with element area and this value, $I_i$, is assigned as the magnitude of the point current source, $\vec{I}$, which is assumed to be placed in the center of gravity of that element. The direction of this current source is the same as the current density direction in the element. Magnetic field at any field point $(x, y, z)$ is then calculated as

$$\vec{B} = \frac{\mu_o}{4\pi} \sum_{i=1}^{450} \frac{\vec{I} \times \vec{R}}{R^3} \tag{6}$$

where $\vec{R}$ is defined from source point $(x', y', z')$ to the field point $(x, y, z)$, $R$ is the magnitude of $\vec{R}$ , and $\mu_o$ is the permeability of free space. Magnetic field is calculated for each element at the center of gravity of that element. In order to avoid the singularity problem encountered in the summation, the effect of element on itself is assumed to be zero. As a result the relation

$$\mathbf{b} = \mathbf{C}\phi \tag{7}$$

is obtained where, $\mathbf{b}$ $(450 \times 1)$ is the vector of magnetic fields calculated for each element at the center of gravity of that element, and $\mathbf{C}$ $(450 \times 256)$ is the matrix relating $\mathbf{b}$ to $\phi$. The elements of $\mathbf{C}$ depend on the mesh properties. Since $\phi$ is a nonlinear function of conductivity distribution, $\mathbf{b}$ is also a nonlinear function of it, i.e.

$$\mathbf{b} = \mathbf{f}(\sigma) \tag{8}$$

## 2.3. Formulation and Solution of the Inverse Problem

Inverse problem is the problem of finding $\mathbf{f}^{-1}$, i.e. finding $\sigma$ for a measured $\mathbf{b}$. Since $\mathbf{f}$ is non-linear and for which an analytical inverse cannot easily be found, this study is confined to finding $\sigma$ perturbation for

a given perturbation in $\mathbf{b}$, i.e. $\mathbf{f}$ is linearized around a background $\sigma_o$. The relation between conductivity and magnetic field perturbations can be written in a matrix form as:

$$\Delta\mathbf{b} = \mathbf{S}\Delta\sigma \tag{9}$$

where vector $\Delta\mathbf{b}$ contains the perturbations in magnetic field measurements, $\Delta\sigma$ is the perturbation in element conductivity values and $\mathbf{S}$ $(450 \times 450)$ is the coefficient matrix named as *sensitivity matrix*. The matrix equation can be written as,

$$\begin{bmatrix} \Delta b_1 \\ \Delta b_2 \\ \vdots \\ \Delta b_m \end{bmatrix} = \begin{bmatrix} \frac{\partial b_1}{\partial \sigma_1} & \frac{\partial b_1}{\partial \sigma_2} & \cdots & \frac{\partial b_1}{\partial \sigma_n} \\ \frac{\partial b_2}{\partial \sigma_1} & \frac{\partial b_2}{\partial \sigma_2} & \cdots & \frac{\partial b_2}{\partial \sigma_n} \\ \vdots & \vdots & \ddots & \vdots \\ \frac{\partial b_m}{\partial \sigma_1} & \frac{\partial b_m}{\partial \sigma_2} & \cdots & \frac{\partial b_m}{\partial \sigma_n} \end{bmatrix}_{\sigma=\sigma_o} \begin{bmatrix} \Delta\sigma_1 \\ \Delta\sigma_2 \\ \Delta\sigma_3 \\ \vdots \\ \Delta\sigma_n \end{bmatrix} \tag{10}$$

Here, $m = 450$ is the number of measurements and $n = 450$ is the number of elements. The first column of the sensitivity matrix corresponds to change in magnetic field in all measurement points when the conductivity of the first element is changed only. Therefore, if the forward problem is solved for an initial conductivity distribution and then solved again by changing the conductivity of first element by a small amount, the difference of two solutions divided by the perturbation in conductivity is the first column of the desired coefficient matrix. This procedure can be repeated for all elements and the sensitivity matrix can be formed. Note again that, the forward problem is linearized around the chosen initial conductivity distribution using this approach. Therefore, inverse problem in this study is defined as solving the above matrix equation.

In order to understand the performance of the imaging system, the sensitivity matrix calculated as above can be analysed using singular value decomposition (SVD) [11]. Using SVD matrix $\mathbf{S}$ is decomposed as:

$$\mathbf{S} = \mathbf{U}\mathbf{\Lambda}\mathbf{V}^{\mathbf{T}} \tag{11}$$

where $\mathbf{U}$ and $\mathbf{V}$ are two orthonormal matrices whose columns are left and right singular vectors respectively and $\Lambda$ is a diagonal matrix with entries $\lambda_i$, $i^{th}$ singular value. The ratio of highest singular value to the lowest one is defined as the condition number and is a measure of singularity. If condition number is defined as:

$$\kappa = \frac{\lambda_{max}}{\lambda_{min}} \tag{12}$$

$\mathbf{S}$ is said to be an ill-conditioned matrix for large $\kappa$.

The sensitivity matrix is calculated and stored for the initial conductivity distribution only. Once the sensitivity matrix is obtained, since $\Delta\mathbf{b}$ is known, desired conductivity perturbation values can be calculated by matrix inversion and multiplication. However, $\mathbf{S}$ is not necessarily square and it is generally singular, thus direct matrix inversion can not directly be applied. For this reason, generalised matrix inverse (or pseudo-inverse) is taken and $\Delta\sigma$ is calculated as:

$$\Delta\sigma = \mathbf{S}^{\dagger}\Delta\mathbf{b} \tag{13}$$

where $\mathbf{S}^{\dagger}$ is the generalised inverse. This inverse can be computed using the singular value decomposed form of $\mathbf{S}$. Since $\mathbf{U}$ and $\mathbf{V}$ are orthonormal matrices, their inverses can simply be obtained by taking their transposes. $\Lambda$ is a diagonal matrix and its inverse is obtained by replacing diagonal entries, $\lambda_i$, with

$1/\lambda_i$. Using these properties and replacing $\mathbf{S}^\dagger$ in Equation (12) desired conductivity change values can be calculated as:

$$\Delta\sigma = \mathbf{V}\Lambda^{-1}\mathbf{U}^T\Delta\mathbf{b} \tag{14}$$

This matrix multiplication can be written in summation form as:

$$\Delta\sigma = \sum_{i=1}^{r} \lambda_i^{-1}\mathbf{v}_i\mathbf{u}_i^T\mathbf{b} \tag{15}$$

where $\mathbf{u}_i$ and $\mathbf{v}_i$ are the columns of matrices $\mathbf{U}$ and $\mathbf{V}$ and they can also be called as measurement basis vectors, and image basis vectors respectively. In this summation, if there exists some $\lambda_i$ very close to zero, some values of $\Lambda^{-1}$ will grow drastically and cause errors in the reconstructed image. In order to prevent this, singular vectors corresponding to small singular values are excluded in image reconstruction and this process is named as *truncation*. The optimum truncation level depends on the object to be imaged and the noise level.

## 3. Results

In order to understand the performance of the suggested reconstruction algorithm, simulation studies were undertaken. For this purpose a FEM model for the phantom described in Figure 1 is developed (Figure 2). It is assumed that the phantom is two dimensional because it is thin compared to its other dimensions and current injection electrodes have the same thickness. The FEM model has 256 nodes and 450 first order triangular elements.

To understand the spatial resolution that can be achieved by the proposed algorithm, the behaviour of the point spread function of this imaging system is analysed. For this purpose, point objects are placed in different parts of the imaging region. The background conductivity is selected as 0.002 S/m in all simulations. Images obtained for a point object with 0.00202 S/m conductivity and of size $0.6cm \times 0.56cm$ (covering two neighbouring finite elements which constitutes a rectangular pixel) placed in central, intermediate, or peripheral regions are presented in Figure 3. These images have well defined peaks corresponding to the exact locations of the point objects and the full-width- half-maximum (FWHM) values of these peaks are less than one pixel, irrespective of the position of the object. Therefore, it can be argued that ultimate spatial resolution is achieved uniformly throughout the imaging region within the limits of the finite element mesh used. In injected EIT very high degree of smearing is observed in reconstructed images. For example, for a 1 cm diameter circular object close to the periphery, a 3.6 cm diameter (FWHM) is obtained. Furthermore, in central regions smearing is worse [17]. It is also observed that peak values of conductivity calculated are $1.85 \times 10^{-5}\ S/m, 1.84 \times 10^{-5} S/m$ and $1.79 \times 10^{-5} S/m$ for central, intermediate, and peripheral cases respectively and these values are only 10% less than the peak of the actual point object. In injected EIT, however, the reconstructed images are highly attenuated and about 10% of the actual peak values are obtained[17].

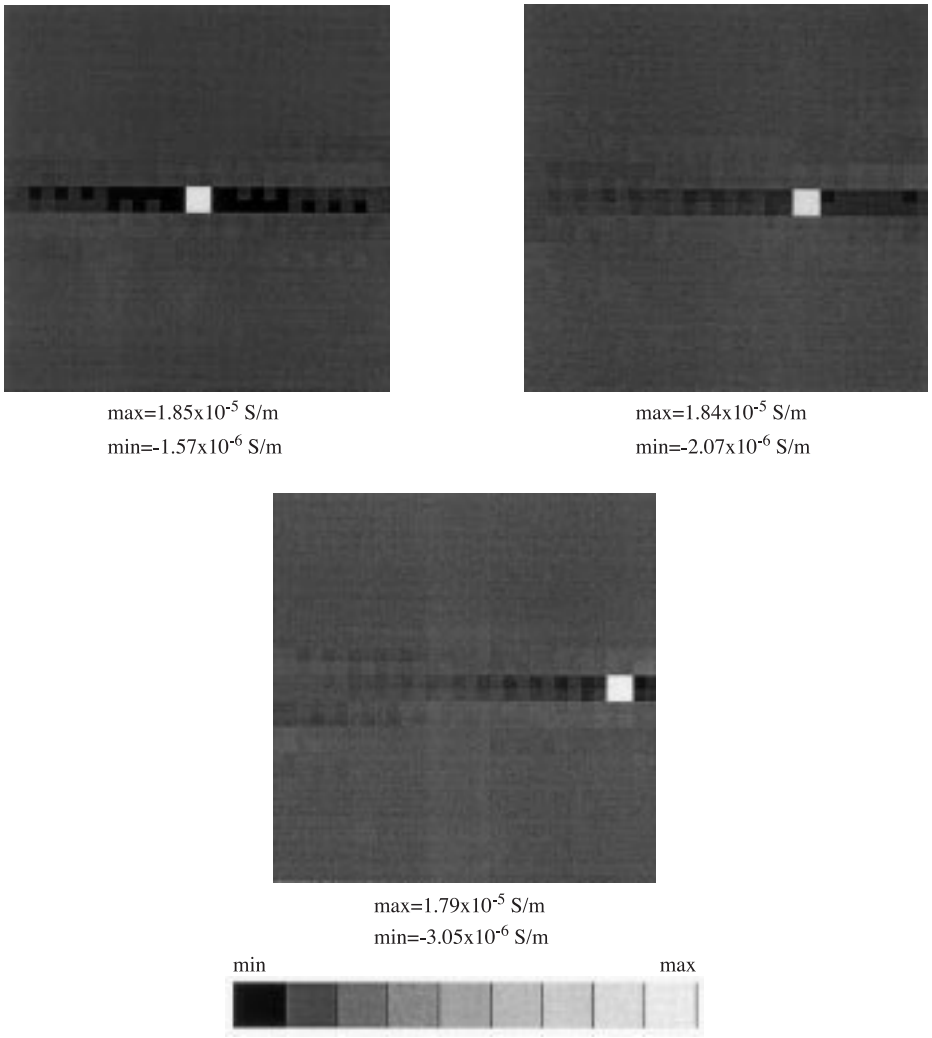


**Figure 3.** Images reconstructed for objects placed in central, intermediate and peripheral regions. The width and length of the objects are 0.6cm and 0.56cm respectively. No truncation is done during reconstruction. The values in the images show the deviation from background conductivity. Background conductivity is 0.002S/cm for all cases.

In Figure 4, an artifact, which we have named "horizontal strip" artifact is observed. In this figure "horizontal" corresponds to the x-direction as defined in Figure 1. This artifact is perpendicular to the injected current direction. Since the applied current does not have an x-dependence, variation of conductivity only in the y-direction, does not alter the current distribution and the resulting magnetic field. Consequently, it may be conjectured that, some image basis vectors which vary only in the y-direction will have very small corresponding singular values. Indeed, it is observed that there are quite a few such image basis vectors with very low singular values and these basis functions appear to have abrupt step variations in the y-direction. The horizontal strip artefact is probably due to the contributions of such image basis functions.

An object with high contrast ($\sigma = 0.004 S/m$) is placed in the imaging region and the reconstructed image is compared with the case in which an object with low contrast is placed in the same place. The images reconstructed for low and high contrast cases are given in Figure 4. In this figure, it is seen that the object can easily be resolved for both cases but the conductivity value in high contrast case is 30% less than the actual value. It must be noted that even this 30% error represents a major improvement over the

results obtained by conventional EIT techniques [17]. This result shows that, even though a linearization procedure is applied in obtaining the sensitivity matrix, in which the conductivity distribution is assumed to be incrementally perturbed, the resulting reconstruction algorithm applies quite satisfactorily for high contrast objects as well.

Images using simulated data for some representative cases are also obtained. Two rectangular objects of size $1.13cm \times 1.20cm$ with centers of gravity (-2cm,2.5cm) and (2cm,-1.5cm) are placed in the imaging region. Both of the objects are insulator objects with conductivity $0.00002S/m$ (1% of the background conductivity). In Figure 5 (a) the image reconstructed with no truncation is given. The two objects can not be resolved for this case. However, when last 4 singular values are truncated Figure 5 (b)) the objects can easily be observed with correct dimension and placement. Therefore, suggested imaging algorithm gives satisfactory output images for more complex conductivity distributions as well.

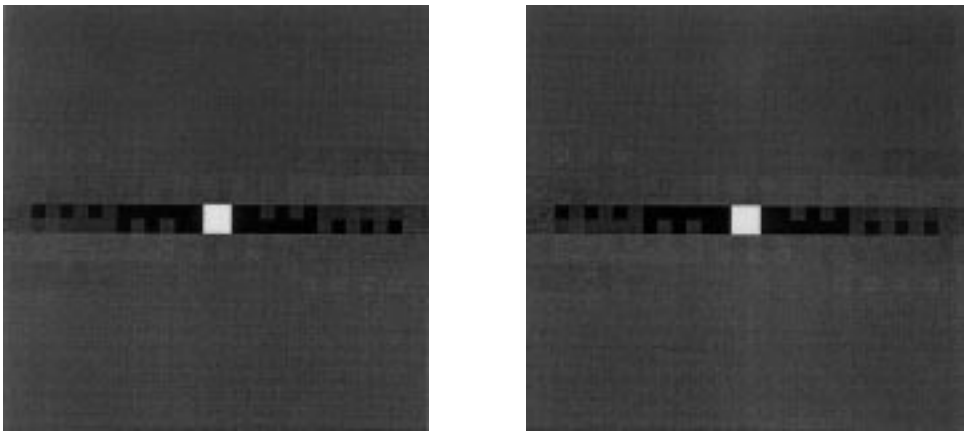


**Figure 4.** Images obtained for low and high contrast objects. Background conductivity is 0.002S/m. Conductivity of the objects in (a) and (b) are 0.00202S/m and 0.004 S/m respectively.

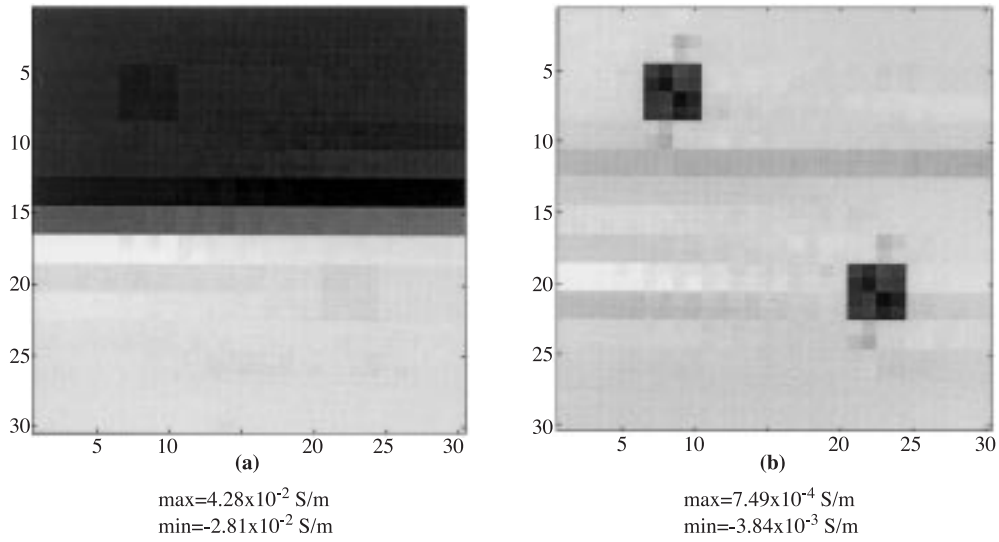


**Figure 5.** Images obtained for double object case. Both objects are insulator with conductivity of $0.00002S/m$.

Size of the objects is $1.13cm \times 1.20cm$. Their centers are at (-2cm, 2.5cm) and (2cm,-1.5cm). (a) No truncation (b) Last 4 singular values are truncated.

After understanding the performance of the suggested imaging technique and reconstruction algorithm using simulated data, some images using experimental data are obtained. The details of experimental set-up and data acquisition strategy are given in 6. For two insulating disk objects placed in the imaging region (the radii of the two objects are both 0.75 cm and their centers are at (-2cm, 2.5cm) and (2cm, -1.5cm)) the magnetic field measured using MRI is used for reconstruction (measurement data are taken from [10]). The images obtained with and without truncation are shown in Figure 6. The two objects are again well identified. In Figure 6 (b), 2 singular vectors are truncated and by this way the high contrast noisy behaviour on the lower left corner of Figure 6 (a) is avoided and object contrast is enhanced. In the reconstructed image, objects appear to be shifted with respect to their actual positions (centers of the objects in the reconstructed image are found to be (-2.6cm,1.89cm) and (0.8cm, -1.82cm)). The magnetic field data used in these reconstructions were very noisy [10]. Furthermore, the sampling rate of the magnetic field was almost half of the sampling rate of the conductivity distribution as realized by our specific mesh structure. Also it is likely that there are shifting and scale errors in the data used. Therefore, Figure 6 can be considered to represent the result of a preliminary study at this stage; nevertheless, it demonstrates that the MR-EIT technique proposed in this study is feasible. To test if one can obtain accurate contrast and high resolution images using real data, it is necessary to make reconstructions using less noisy and more accurate magnetic field measurements.

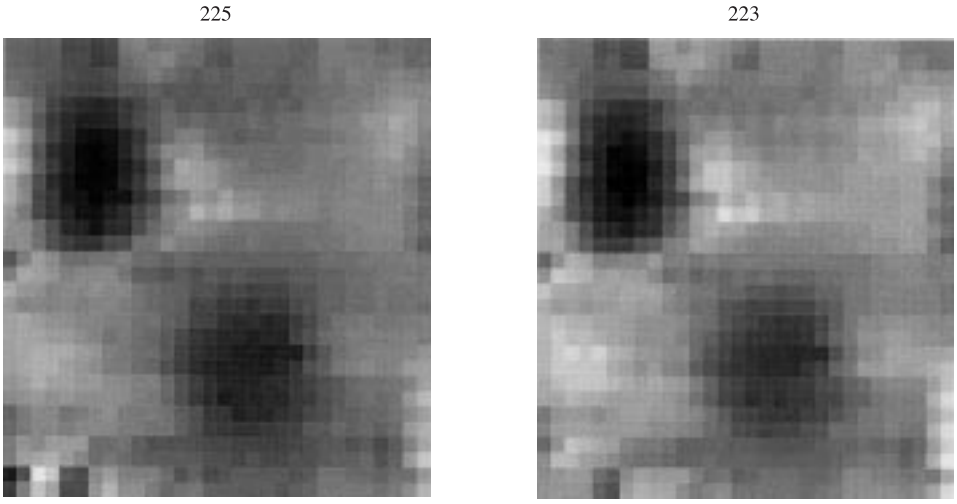


**Figure 6.** Images reconstructed using data taken from experimental phantom. In (a) no truncation is made. (b) Last 2 singular vectors are truncated.

# 4. Discussions and Conclusion

The results of this study show that it is possible to obtain high-resolution images throughout the whole imaging region using MR-EIT. The results obtained for low and high resolution objects are compared to understand the effect of linearization and it is seen that even for high conductivity perturbations the object can correctly be located with the cost of higher error in peak conductivity value. Finally, experimental results show that the proposed reconstruction algorithm which utilizes magnetic field measurements made using MRI is feasible.

As opposed to injected EIT, it is possible to increase number of measurements without increasing the number of electrodes, thus, conductivity images with high resolution can be obtained. It is also possible to increase the number of measurements by repeating magnetic field measurements for different current injection patterns.

3-D extension of the proposed method is necessary in order to obtain images from the human body. Last but not least, improvements in magnetic field measurements using MRI will significantly contribute to the quality of the MR-EIT images.

# References


[1] D C Barber, B H Brown, and I L Freeston, "Imaging Spatial Distribution of Resistivity using Applied Potential Tomography," *Electronic Letters*, vol. 19, pp. 933-935, 1983.

[2] D C Barber and B H Brown, "Applied Potential Tomography," *J. Phys. E. Sc. Instrum*, vol. 17, pp. 723-733, 1984.

[3] W R Purvis, R C Tozer, and I L Freeston, "Impedance Imaging Using Induced Currents," *IEEE EMBS 12th Ann. Int. Conf. Proc.*, pp. 114, 1990.

[4] N G Gençer, Y Z İder, and M Kuzuoğlu, "Electrical Impedance Tomography Using Induced and Injected Currents," *Clin. Phys. Physiol. Meas.*, vol. 12, suppl. A pp. 95-99, 1992.

[5] N G Gençer, Y Z İder, and M Kuzuoğlu, "Electrical Impedance Tomography Using Induced Currents," *IEEE Transactions on Medical Imaging*, vol.13 pp. 338-350, June 1994.

[6] G C Scott, R L Armstrong, and R M Henkelman, "Magnetic Field Measurement by NMR Imaging," *IEEE Transactions on Medical Imaging*, vol. 10 pp. 362-374, 1991.

[7] Y Z İder, L T Müftüler, and Ö Birgül, "Use of MRI for Measuring AC Internal Currents of EIT: A Feasibility Study," *Proc. of IXth International Conference on Electrical Bio-Impedance in conjunction with European Concerted Action on Impedance Tomography*, pp. 420-422, September 1995.

[8] L T Müftüler and Y Z İder, "Measuring AC Magnetic Field Distribution using MRI," *Proc. of IEEE Engineering in Medicine and Biology 18th Annual International Conference*, 1996.

[9] P P Silvester and R L Ferrari, "Finite Elements for Electrical Engineers," *Cambridge University Press*, 1983.

[10] L T Müftüler, "Measurement of Magnetic Field Generated by Nonuniform AC Current Density using Magnetic Resonance," *Ph. D. Thesis in EE Eng.*, METU, 1996.

[11] G H Golub and C F van Loan, "Matrix Computation," *The John Hopkins University Press*, 1983.

[12] Ö Birgül and Y Z İder, "Use of Magnetic Field Generated by the Internal Distribution of Injected Currents for Electrical Impedance Tomography," *Proc. of IXth International Conference on Electrical Bio-Impedance in conjunction with European Concerted Action on Impedance Tomography*, pp. 418-419, September 1995.

[13] Ö Birgül and Y Z İder, "Electrical Impedance Tomography Using Magnetic Field Generated by Internal Current Distribution," *Proceedings of IEEE Engineering in Medicine and Biology, 18th Annual International Conference*, 1996.

[14] Ö Birgül, "Electrical Impedance Tomography Using Magnetic Fields Generated by Injected Currents," *MSc. Thesis in EE Eng.*, METU, 1997.

[15] Ö Birgül, Y Z İder, and N G Gençer, "MRI-EIT için Duyarlılık Matrisinin Türetilmesi," *TMMOB Elektrik Mühendisleri Odası Elektrik-Elektronik Bilgisayar Mühendisliği 7. Ulusal Kongresi Bildiri Kitapçığı*, pp. 168-171, 1997.

[16] Y Z İder and L T Müftüler, "Measurement of Magnetic Field Generated by Non-Uniform AC Current Density Using Magnetic Resonance," *IEEE Transaction on Medical Imaging*, vol. 16 no. 15, pp. 617-622, October 1997.

[17] Y Z İder, B M Eyüboğlu, M Kuzuoğlu, K Leblebicioğlu, U Baysal, B K Çağlar, and Ö Birgül, "A Method for Comparative Evaluation of EIT Algorithms Using a Standard Data Set," *Physiol. Meas.*, suppl. A vol. 16, pp. 227-236, 1995.